Size Effects and Stochastic Behavior of Nanoindentation Pop In

J. R. Morris, H. Bei, G. M. Pharr, and E. P. George

Phys. Rev. Lett. **106**, 165502 — Published 20 April 2011

DOI: 10.1103/PhysRevLett.106.165502

Size effects and stochastic behavior of nanoindentation pop-in

J. R. Morris,[1,2] H. Bei,[1] G. M. Pharr,[2,1] E. P. George[1,2]

[1] Materials Science and Technology Division, Oak Ridge National Laboratory, Oak Ridge, TN 37831-6115

[2] Department of Materials Science and Engineering, University of Tennessee, Knoxville, TN 37996-2200

Abstract:

A statistical model for pop-in initiated at pre-existing dislocations during nanoindentation is developed to explain size-dependent pop-in stresses. To verify theoretical predictions of this model, experiments were performed on single-crystal Mo, utilizing indenter radii that vary by over three orders of magnitude. The stress where plastic deformation begins ranges from the theoretical strength in small volumes, to one order of magnitude lower in larger volumes. An intermediate regime shows wide variability in the stress to initiate plastic deformation. Our theory accurately reproduces the experimental cumulative probability distributions, and predicts a scaling behavior that matches experimental behavior.

A size effect manifested as "smaller is harder" behavior is well known in the indentation literature [1]. For example, hardness is found to increase with decreasing indentation depth for Berkovich indenters [2-3] and decreasing indenter radius for spherical indenters [4-5]. Mechanistically, it has often been attributed to the hardening by geometrically necessary dislocations needed to accommodate plastic strain gradients [2-5]. Similar size-dependent strength has been observed in other specimen geometries where plastic strain gradients are present such as bending [6] and torsion [7].

Recently, a different type of indentation size effect (ISE) was discovered in single crystal Ni [8]. This ISE is based on the stress needed to *initiate* dislocation plasticity (yielding), rather than hardness, which includes contributions from both yielding and work hardening. For a wide range of spherical indenter radii [8], the transition from elastic to plastic behavior occurs with a clear sudden displacement burst in an otherwise continuous load-displacement curve, called a "pop-in" (see Fig. 1a). The maximum shear stress under the indenter at first pop-in (the "pop-in stress") was found to be very high, on the order of the theoretical strength ($\sim G/14$) for small spheres and decreased with increasing indenter radius. Mechanistically, these observations were explained as follows. For sufficiently small indenters, the material in the highly stressed zone underneath the indenter is likely to be dislocation-free, requiring dislocation nucleation at the theoretical stress. As the indenter radius increases, there is an increasing likelihood that a nearby dislocation assists in the onset of plasticity. When a sufficiently large volume of material is probed, plasticity tends to be initiated by the motion of pre-existing mobile dislocations rather than by the nucleation of new dislocations. Thus, the relevant length scales are set by the dislocation density and indenter radius. Consistent with this, when the Ni was pre-strained before indentation (dislocation density increased), the pop-in stresses were found to decrease [8].

The present work experimentally demonstrates the full crossover from pop-in near the theoretical strength at small radii, through a stochastic regime at larger radii, and into a "deterministic" regime for the largest radii where the maximum stress at pop-in is again well defined but much smaller than for the smallest radii. We demonstrate that a stochastic model of plasticity initiated at pre-existing dislocations can accurately describe the mechanism discussed above and predict a distribution of pop-in strengths, particularly in the intermediate regime where experiments give large scatter in the results. This distribution is fundamentally different from that treated in previous work where pre-existing defects are neglected [9].

Nanoindentation experiments were performed on a (100) Mo single crystal using spherical indenters with radii from 700 μm down to 115 nm. The indentation geometry is shown schematically in the inset of Fig. 1a. A spherical tip with radius *R* is indented to a depth *h* by an applied force *F*. Assuming that the material is elastically isotropic and behaves according to Hertzian theory [10], the indenter has a contact radius *a* with the material, given by

$$a = \left(\frac{3FR}{4E_r}\right)^{\frac{1}{3}} \tag{1}$$

where E_r is the reduced Young's modulus given by

$$\frac{1}{E_r} = \frac{1-\nu_s^2}{E_s} + \frac{1-\nu_i^2}{E_i}\,. \tag{2}$$

Here, E_i and E_s are the moduli of the indenter and specimen, respectively; similarly, ν_i and ν_s are the Poisson ratios for the indenter and the specimen. The maximum resolved shear stress τ_{max} in our Mo specimen is related to the indenter radius *R* and the force *F* on the indenter by

$$\tau_{max} = \alpha\left(\frac{6FE_r^2}{\pi^3R^2}\right)^{\frac{1}{3}} \tag{3}$$

where α=0.31 for materials with a Poisson ratio close to 0.3. The indenters used in the present study were made of diamond (R from 115 nm to 64 μm) and sapphire (85-700 μm). The polycrystalline average Young's modulus and Poisson's ratio are 327 GPa and 0.3 for Mo [11], 1141 GPa and 0.07 for diamond [11], 345 GPa and 0.2 for sapphire [12].

A characteristic load-displacement curve is shown in Fig. 1a for R=210 nm. At small loads, the displacement is Hertzian, and the system can be unloaded reversibly. At a load near F=0.4 mN, a sudden large displacement occurs, and the material is plastically deformed. This pop-in is presumably accompanied by the generation and motion of many dislocations to accommodate the resultant strain. A permanent hardness impression remains in the surface after unloading. Using Eq. 3, pop-in occurs when the peak resolved shear stress reaches a value of τ_{max}=16.3 GPa, close to the theoretical strength of 15 GPa predicted from first-principles [10, 13].

Repeated experiments with this indenter produced a relatively tight distribution of pop-in stresses, Fig. 1b. Similar distributions, close to the theoretical strength, were obtained for two other small indenters (R = 115 and 580 nm). One explanation for these pop-ins is that they were initiated by the *homogeneous* nucleation of dislocations Additionally, if the tip is truly spherical, and the surface is perfectly smooth and clean of any oxide or other layer, then a distribution such as that shown in Fig. 1b is likely due to thermal fluctuations. Indeed, thermally-activated homogeneous nucleation has been used to explain the distribution of pop-in loads and effects of different strain rates [9, 14]. Surface roughness and oxide or other surface layers can also contribute to a variation in pop-in activation barriers, particularly for the smallest indenters [15-16]. As our results for the three different small radii give very similar distributions, we conclude that these other effects are negligible.

For larger indenters, with relatively large stressed regions, there is some likelihood that pre-existing dislocations near the indenter will affect the pop-in stress. To investigate this, nanoindentation experiments were conducted for a range of indenter sizes, with 36 indentations per indenter radius. For R<200 μm, all tests showed clear pop-ins. However, for the two larger indenters (~209 and ~700 μm), 3-5 (out of 36 for each indenter) did not show clear pop-in. Figure 2 presents the cumulative pop-in probability, as a function of τ_{max} for the various indenter sizes down to R = 0.58 μm (for clarity, data for the two smallest indenters, R = 0.21 and 0.115 μm, which overlap those for R = 0.58 μm, are not shown). The cumulative probability $P_{pop\text{-}in}(R;\tau_{max})$ is the probability that a pop-in occurs before the maximum shear stress reaches a value τ_{max}, for an indenter of size R. For R=0.58 μm, the probability of pop-in is small until τ_{max} is close to the theoretical value, suggesting that the probed volume in this case is very likely dislocation-free. For the largest radius (700 μm), the probability of pop-in rapidly changes from 0 to 1 as τ_{max} approaches 0.5 GPa, ~30 times smaller than the small-radius value. In this case, the probed volume is large, and likely contains many dislocations. For intermediate radii, the cumulative probability becomes quite broad: for R=6.62 μm, the value of τ_{max} where pop-in occurs ranges from ~2 to 14 GPa. These are significantly higher than any of the values for R=700 μm, yet the largest pop-in stress is smaller than the theoretical strength.

We develop a simple stochastic model of this behavior, assuming that there are local dislocation configurations in the Mo single crystal that give rise to pop-in. These may be dislocation pinning points, dislocation junctions, or locally pinned dislocation segments acting as a Frank-Read source. The model does not differentiate among these possibilities, but treats them as point defects with some density (per volume), ρ_{def} in the initial material, whose positions are completely uncorrelated. We further assume that, if a defect is subjected to a shear stress $\tau_{\text{pop-in}}$, pop-in will occur. The value of $\tau_{\text{pop-in}}$ is assumed to be the same everywhere. In reality, there will be some distribution of values arising from several factors including different activation strengths for different dislocation configurations, local stress concentrations from surface imperfections, and from variations due to thermal activation. Thermally activated processes are neglected in our athermal model, but are relevant for understanding strain-rate effects, as well as observations that a short-time hold can produce plastic events at smaller stresses [15-16].

The probability $P_0(R;\tau_{max})$ that pop-in has *not* occurred when the maximum shear stress has a value of τ_{max} is the probability that there are no defects in the highly stressed region where $\tau > \tau_{\text{pop-in}}$. The cumulative probability is then

$$P_{pop\text{-}in}(R;\tau_{max}) = 1 - P_0(R;\tau_{max}). \quad (4)$$

The situation may be envisioned using the schematic inset in Fig. 3. The volume where the stress is higher than $\tau_{\text{pop-in}}$ is inside the indicated contour. If there is at least one defect in that region, pop-in will occur. If there is no defect, and the maximum stress is less than the theoretical strength, no pop-in will occur.

To calculate the cumulative probability, we define the volume $V(R;\tau_{max;}\ \tau_{\text{pop-in}})$ as the region where the local resolved shear stresses satisfy $\tau > \tau_{\text{pop-in}}$, assuming purely elastic conditions. This volume depends on the radius of the indenter, and on the maximum shear stress under the indenter. If there is at least one defect in that volume, then pop-in will occur. Consider the probability $P_0(V)$ that the volume V has no defects. The assumption of uncorrelated defects allows us to use the results of Poisson (or exponential) statistics to predict that

$$P_0(V) = \exp\left(-\rho_{def}V\right). \quad (5)$$

The cumulative probability is therefore

$$P_{pop\text{-}in}(R;\tau_{max}) = 1 - \exp[-\rho_{def}V(R;\tau_{max;}\ \tau_{\text{pop-in}})]. \quad (6)$$

Thus, given ρ_{def} and $\tau_{pop\text{-}in}$, the cumulative probability of pop-in may be calculated for any given combination of indenter radius and maximum stress under the indenter.

The stress field under the indenter may be calculated directly from Hertzian contact theory [10]. All lengths may be scaled in terms of the contact radius a of the indenter with the surface, and the stresses scale with the maximum shear stress τ_{max} under the indenter. We express the scaled volume for all conditions in terms of a single function:

$$V/a^3 = f(\tau_{pop\text{-}in}/\tau_{max}). \quad (7)$$

This dimensionless function is plotted in Fig. 3. When $\tau_{pop\text{-}in} > \tau_{max}$, the volume is zero as expected: the stress everywhere is less than that to initiate pop-in at a pre-existing dislocation. As τ_{max} increases above $\tau_{pop\text{-}in}$, the volume rapidly grows.

With the above assumptions, the cumulative probability $P_{pop\text{-}in}(R;\ \tau_{max})$ may be calculated. In the large indenter limit, where the spread in the pop-in stress is small, the average pop-in stress is assumed to determine the defect strength: we set $\tau_{pop\text{-}in}$ equal to the average experimental pop-in stress for the largest indenter (R= 700 μm); specifically, $\tau_{pop\text{-}in}$=0.52 GPa. The defect density was adjusted to fit the rest of the cumulative probabilities, resulting in $\rho_{def}=2\times10^{16}/\text{m}^3$. (The sensitivity of the fits to this value is discussed below.) The predicted cumulative probability curves, shown as solid lines in Fig. 2, are in good agreement with experiments when $R \geq 3.75$ μm. For these radii, the pop-in primarily occurs when τ_{max} is less than the theoretical strength. The theory correctly predicts that for large radii, the pop-in occurs at a well-defined stress, but that for smaller radii the average stress is higher, and the spread increases significantly. The wide variability occurs when the highly stressed region has a volume comparable to the volume per defect ($1/\rho_{def}$). In this case, there is a wide variability that depends on whether or not there is a dislocation in the highly stressed region that may induce pop-in. For the smallest radii, the distribution becomes narrow again, as the pop-in becomes dominated by nucleation mechanisms, independent of the pre-existing dislocation distribution. Note that the relevant scale determining the change to a narrow distribution at small R is the volume of the highly stressed region (determined by R and the applied load), not the contact radius a. Figure 3 shows that this volume may be orders of magnitude larger than a^3.

We now create a scaling theory for the pop-in behavior. Let $\tau_{½}(R)$ be the value of the stress τ_{max} where the cumulative probability is ½ for a given radius. From Eq. (6), $\rho_{def} V = \ln(2)$ at this stress value, and along with Eq. 7, this gives

$$\ln(2)/a^3 = \rho_{def}\, f(\tau_{pop\text{-}in}/\tau_{½}). \qquad (8)$$

Thus, plotting a^{-3} vs. $1/\tau_{½}$ for each radius should give a universal curve with the shape shown in Fig. 3, since the parameters $\tau_{pop\text{-}in}$ and ρ_{def} are material parameters independent of the indenter radius. Figure 4 verifies this behavior, showing both the predicted behavior and experimentally determined values of $\tau_{½}$. For larger radii (≥ 3.75 µm) the data fall close to our theoretical prediction. Dashed lines indicate curves predicted by defect densities that are ±20% of the previously given value. As dislocation densities are typically only determined to within an order of magnitude, this is reasonably precise. This density suggests a typical separation of defects of $\rho_{def}^{-1/3}$=3.7 µm. Assuming a cubic array of dislocation lines with this separation between dislocations gives ρ_{disl}=2.2x10^{11}/m^2. X-ray line broadening measurements on these materials show a value of ρ_{disl}=10^{11}/m^2 [17], with a typical separation of 3.2 µm. Thus, the model produces reasonable numbers. Another interpretation of the defects is that they are dislocation pinning points; comparing the experimental dislocation density and the fitted density, this would give on average one pinning point for every 5 µm of dislocation line length.

Equation 6 indicates that pop-in caused by preexisting dislocations will likely occur when the highly stressed region has a volume on the order of $1/\rho_{def}$. When $V\rho_{def}$>>1, then there is likely a defect assisted pop-in event. Otherwise, there are likely no dislocations in the stressed region, and pop-in requires dislocation nucleation. This is clearly shown in Fig. 4: for sufficiently small radii (≤ 1.5 μm), $\tau_{½}$ shows no pop-in size effect, indicating this is a nucleation-dominated regime. The crossover between the two regimes is determined by ρ_{def}, by the alternate mechanisms at small radii, and possibly by both temperature and indentation rate (through $\tau_{pop\text{-}in}$, assuming that thermal effects are significant.)

A similar effect may be present in other geometries, including micropillars [18]: whenever the highly stressed region has a volume comparable to the volume per defect, a stochastic behavior is to be expected, associated with the number (or absence) of defects and their type in the volume. The behavior is not only dependent on sample size, but also on the defect density. This has been observed in Mo-alloy micropillars [19]. However, the analogy is not perfect because micropillars have nominally uniform stresses throughout; therefore, their stochastic behavior must reflect a *distribution* of defect strengths. For nanoindentation, a single stress at which all the defects are activated is sufficient to produce a reasonable model of the stochastic behavior. This suggests that pillar geometries may allow for a probe of this defect strength distribution.

Acknowledgements: Research sponsored by the U.S. Department of Energy, Office of Basic Energy Sciences, Materials Sciences and Engineering Division.

References:

[1] D. Tabor, *The Hardness of Metals* (Oxford University Press, Oxford, 2000).

[2] W. D. Nix, and H. J. Gao, *J. Mech. Phys. Solids* **46**, 411 (1998).

[3] H. Gao, Y. Huang, W. D. Nix, and J. W. Hutchinson, *J. Mech. Phys. Solids* **47**, 1239 (1999).

[4] J. G. Swadener, E. P. George, and G. M. Pharr, *J. Mech. Phys. Solids* **50**, 681 (2002).

[5] S. Qu, Y. Huang, G. M. Pharr, and K. C. Hwang, *International Journal of Plasticity* **22**, 1265 (2006).

[6] J. S. Stolken, and A. G. Evans, *Acta Materialia* **46**, 5109 (1998).

[7] N. A. Fleck, G. M. Muller, M. F. Ashby, and J. W. Hutchinson, *Acta Metallurgica Et Materialia* **42**, 475 (1994).

[8] S. Shim, H. Bei, E. P. George, and G. M. Pharr, *Scripta Materialia* **59**, 1095 (2008).

[9] C. A. Schuh, and A. C. Lund, *Journal of Materials Research* **19**, 2152 (2004).

[10] K. L. Johnson, *Contact Mechanics* (Cambridge University Press, Cambridge, 1987).

[11] G. Simmons, and H. Wang, *Single Crystal Elastic Constants and Calculated Aggregate Properties: A Handbook* (M.I.T. Press, Cambridge, 1971).

[12] Micro Star Technologies, *Nano Indenters from Micro Star Technologies*, http://microstartech.com/index/NANOINDENTERS.pdf (2011).

[13] S. Ogata, J. Li, N. Hirosaki, Y. Shibutani, and S. Yip, *Phys. Rev. B* **70**, 104104 (2004).

[14] H. Bei, Y. F. Gao, S. Shim, E. P. George, and G. M. Pharr, *Phys. Rev. B* **77** (2008).

[15] W. W. Gerberich, S. K. Venkataraman, H. Huang, S. E. Harvey, and D. L. Kohlstedt, *Acta Metallurgica Et Materialia* **43**, 1569 (1995).

[16] D. E. Kramer, K. B. Yoder, and W. W. Gerberich, *Philos. Mag. A-Phys. Condens. Matter Struct. Defect Mech. Prop.* **81**, 2033 (2001).

[17] R. Barabash, H. B. Bei, and E. P. George, *in preparation*.

[18] M. D. Uchic, D. M. Dimiduk, J. N. Florando, and W. D. Nix, *Science* **305**, 986 (2004).

[19] H. Bei, S. Shim, G. M. Pharr, and E. P. George, *Acta Materialia* **56**, 4762 (2008).

Figure captions.

Fig. 1. (Color online) (a) Schematic of the indentation geometry just before pop-in for a spherical indenter with radius *R* and contact radius *a* with an indentation depth *h*; and a characteristic load-displacement curve for the *R*=210 nm indenter. Assuming isotropic elasticity, the maximum resolved shear stress under the indenter occurs at a depth of 0.48 *a*. (b) Cumulative probability of pop-in, as a function of maximum stress under the indenter, for the *R*=210 nm indenter.

Fig. 2. (Color online) Cumulative probability of pop-in, as a function of maximum stress under the indenter, for a series of indenter radii (points). Smooth curves show the predicted behavior. The dashed vertical line indicates the theoretical strength (τ_{theo}), where dislocation generation may occur without a pre-existing defect.

Fig. 3. (Color online) Calculated volume of the highly stressed region, where the shear stress exceeds the defect-driven pop-in strength.

Fig. 4. (Color online) Comparison of experiment with the scaling theory. Points (labeled by indenter size in µm) show the experimental values of maximum stress under the indenter, where the cumulative probability of pop-in is 50%. Solid curve shows the theoretical prediction, for a defect density of ρ_{def}=2.0×10^{16}/m^3. Dashed curves show results for ρ_{def}=1.6×10^{16}/m^3 and ρ_{def}=2.4×10^{16}/m^3.

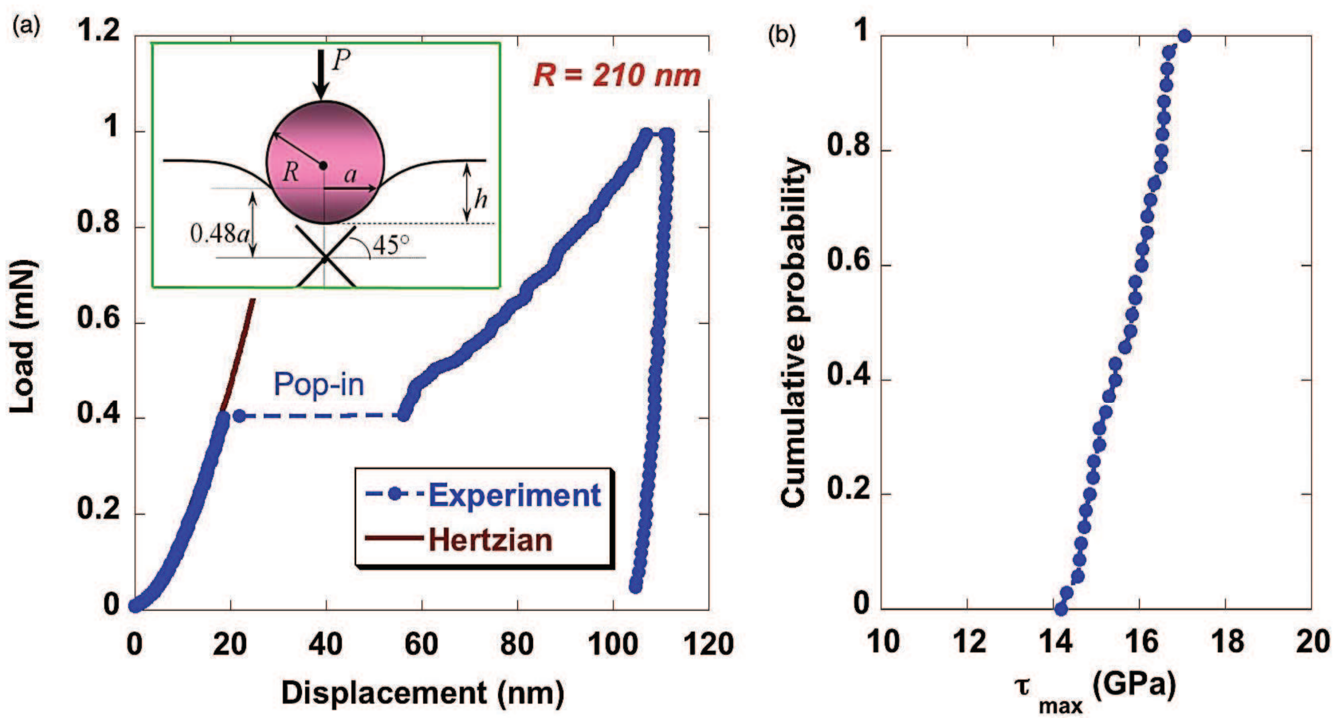

Figure 1 LZ11896 21MAR2011

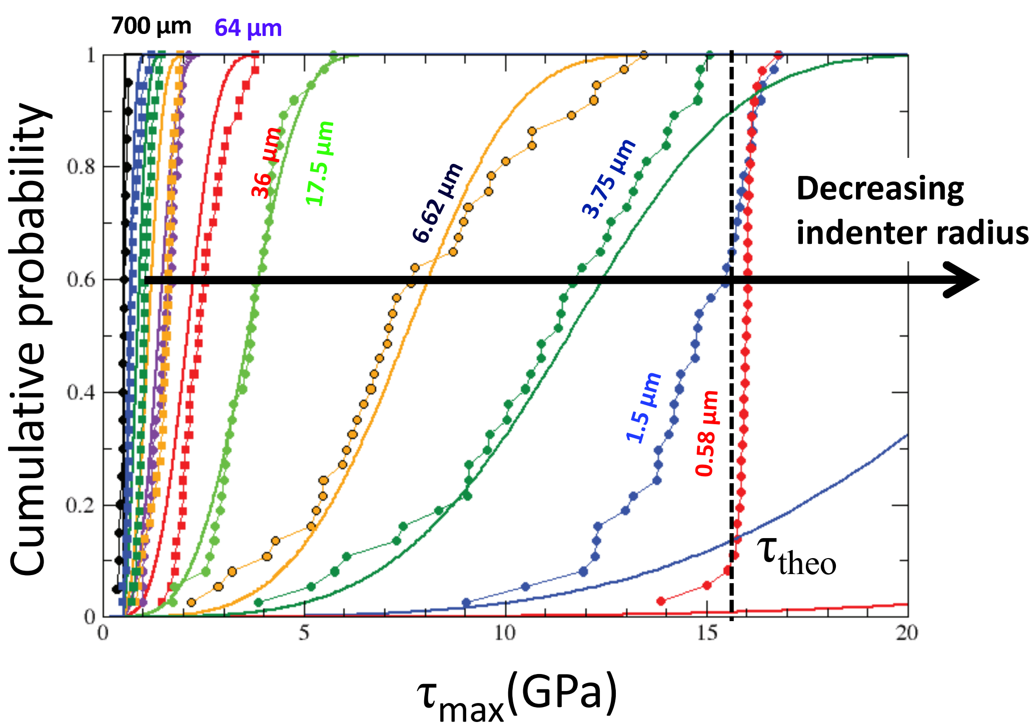

Figure 2 LZ11896 21MAR2011

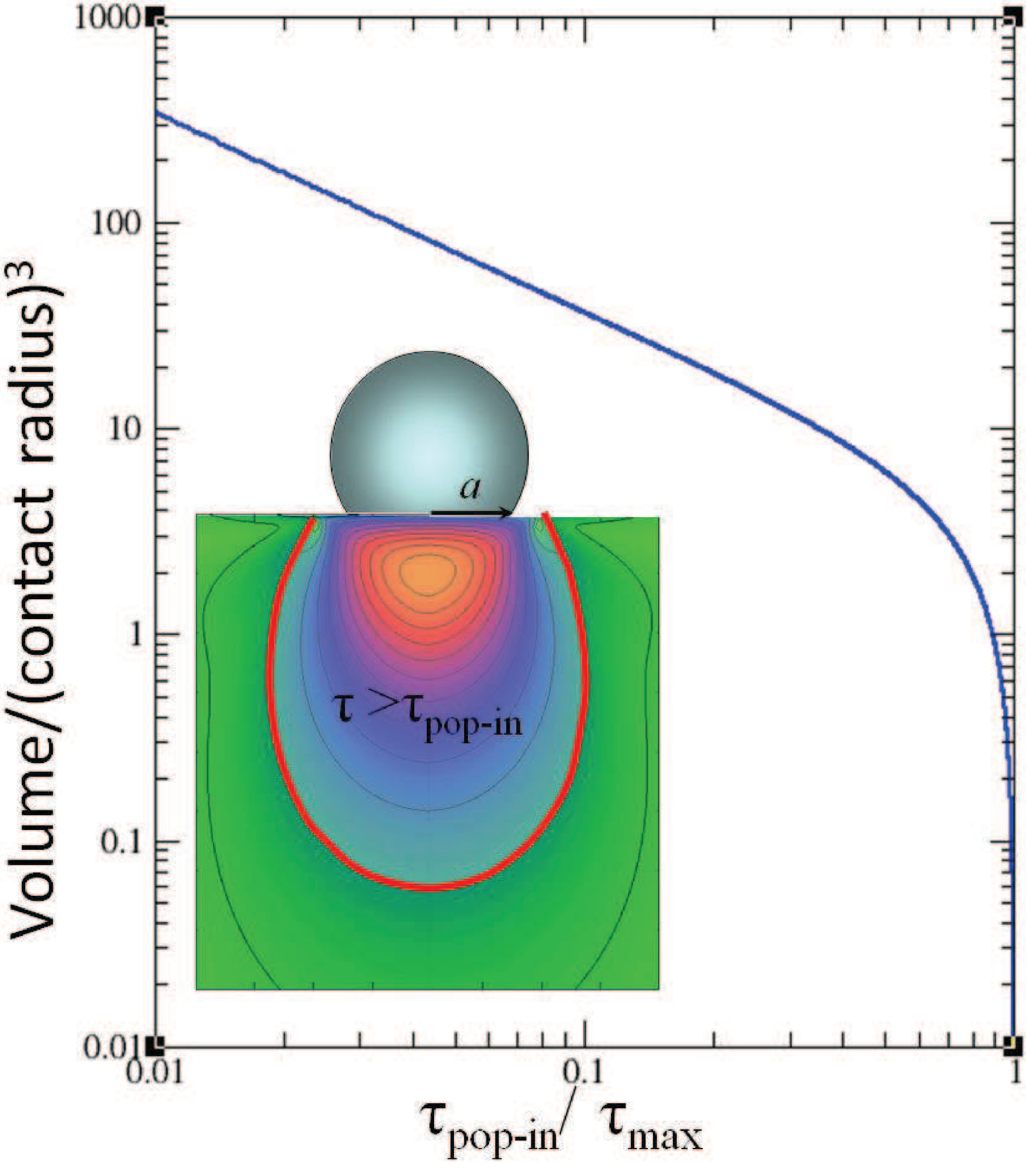

Figure 3 LZ11896 21MAR2011

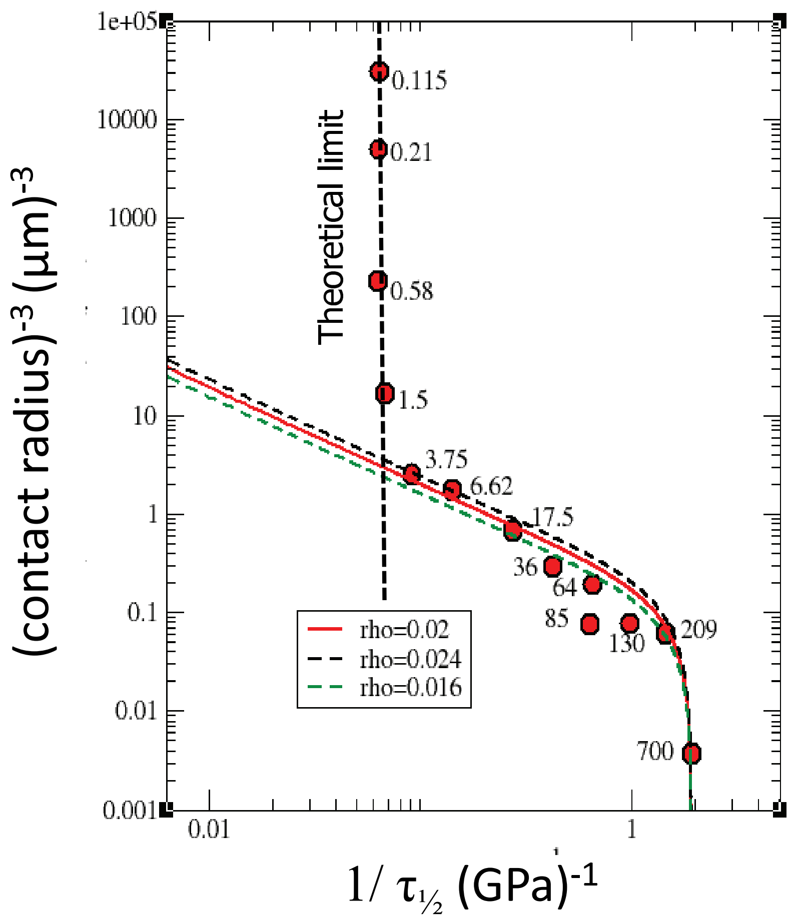

Figure 4 LZ11896 21MAR2011